Design of a compact Fresnel system for optimization of industrial processes

Marco Antonio González Martínez[1], María Dolores Durán-García[1] and Eduardo González-Mora[1]

Facultad de Ingeniería, Universidad Autónoma del Estado de México, Toluca (México)

Abstract

The transition to renewable energy requires efficient solar-thermal conversion technologies for industrial applications. Within this field, Linear Fresnel Reflectors (LFRs) are a promising technology for providing medium-temperature process heat. A key challenge lies in optimizing LFR designs to balance optical efficiency, manufacturing cost, and ease of installation for widespread adoption. Here we show that a compact LFR system, incorporating uniformly spaced mirrors and a novel non-imaging M-shaped cavity, achieves high-efficiency steam generation. This optimized configuration demonstrates a significant performance improvement over an initial prototype with a fixed receiver and non-uniform mirror layout. By comparing our design to conventional trapezoidal and compound parabolic concentrator-based cavities, we provide a clear framework for optimizing optical collection and minimizing losses. Our findings establish a practical pathway for decarbonizing industrial heat, a significant source of global carbon emissions. This work underscores the potential for material-efficient and locally manufacturable solar concentrators, offering a replicable model for sustainable energy solutions in regions with high solar insolation.

Keywords: *solar energy, linear Fresnel reflector, solar thermal energy, process heat.*

1. Introduction

Industrial process heat accounts for 67% of the energy demand in Mexico's industrial sector, a demand currently met primarily by natural gas (Payback MÉXICO 2018). Solar Heat for Industrial Processes (SHIP) represents a key opportunity for partial replacement, which would reduce fossil fuel consumption and associated emissions. Among linear solar concentrators, parabolic troughs and linear Fresnel reflectors (LFR) are prominent technologies; however, LFR systems remain largely unexplored in the Mexican context. Although commercial LFRs in other countries can achieve temperatures up to 300 °C, their large physical dimensions pose a limitation. The Figure 1 (b) indicate a high market potential for SHIP in Mexico, but the limited diffusion of LFR technology opens significant research opportunities. This work aims to optimize the physical parameters of a compact LFR system through SolTrace simulations. By modeling the concentrator and evaluating its performance, we seek to contribute an optimized design that facilitates the implementation of this technology within the national industry.

1.1 Background on process heat

Industrial process heat refers to thermal energy used directly in the preparation or treatment of materials for manufacturing. This energy fulfills various needs, including steam generation, drying with hot air, and direct heating (Fred A. Curtis, 1984). The integration of solar thermal energy for industrial processes (SHIP) demonstrably reduces fossil fuel consumption. It supports the transition to a carbon-free economy, driving a growing trend of SHIP projects implementation across diverse industries. Nevertheless, research in this sector remains limited. Recent analyses reveal a scarcity of studies that develop solar integration methodologies for this sector, alongside a comprehensive investigation of suitable integration layouts (Tasmin et al., 2022).

Although SHIP has not yet become a standard solution, the market has achieved considerable volume, as illustrated by the first World Map of Solar Process Heat Specialists in 2017 (Figure 1(a)). Similarly, the Solar Payback project recognized strong market potential for SHIP suppliers in four key countries (Figure 1 (b)). A specific Solar Payback study in Mexico highlights the relevance of SHIP technologies, which can deliver heat up to 400°C, thereby expanding their applicability across industrial sectors. Energy efficiency is crucial for optimizing the profitability of SHIP projects, whose economic viability depends on a thorough analysis of payback periods and return on investment.

10.18086/swc.2025.02.10 Available at http://proceedings.ises.org

In Mexico, the industrial sector accounted for 31% of the nation's final energy consumption in 2016. Within this sector, thermal energy demand constituted 67% of total consumption, while electricity represented only 33% (Figure 1). The industrial heat demand is met almost entirely by fossil fuels, with natural gas as the predominant source (58%) (Payback MEXICO, 2018). This is mainly due to public policies and the availability of technology. The study above also presents the results of a survey of SHIP technology providers in Mexico, as shown in Table 1, which indicates that Fresnel collector technology is not currently offered. This gap represents a significant opportunity for the development of this technology, given its demonstrated capacity to generate medium- and high-temperature process heat.

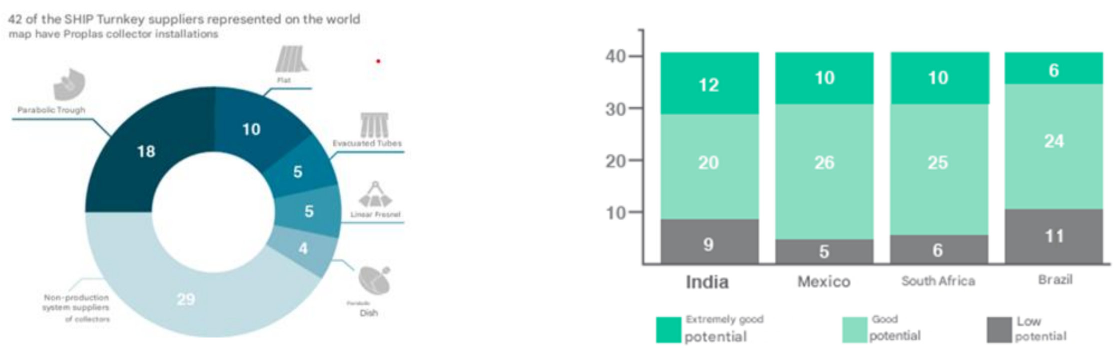

(a) World Solar Process Heat deployment **(b) SHIP markets rating**

Figure 1 . Solar Process heat data (Solar Payback, 2017)

Table 1- The most representative companies offering solar thermal solutions for industry in Mexico (Playback MÉXICO, 2018)

Country	Company	Technologies for process heat
México	Modulo solar	Uncovered, flat, and evacuated tube concentrators
México	Inventi Power	Parabolic trough concentrators
México	Heliocol	Uncovered, flat, and evacuated tube concentrators
México	Tecnosol	Flat concentrators
México	Captosol	Flat concentrators
México	Savosolar /Jorgensen	Flat concentrators
México	Citrus JMk	Parabolic through concentrators (Inventive Power)

1.2 Linear solar concentrators

Linear solar concentrators utilize reflective surfaces to focus solar radiation onto a linear receiver, with parabolic troughs and linear Fresnel reflectors (LFR) representing the two dominant technologies.

1.2.1 Parabolic troughs

Parabolic trough systems (Figure 2) employ a series of parabolic-shaped mirrors that approximate a continuous trough. These mirrors concentrate incoming solar radiation onto a linear receiver positioned at their focal line. The receiver typically consists of a metal tube coated with a selective surface to maximize solar absorption and minimize thermal emissivity. A vacuum-sealed glass cover encloses this absorber tube, significantly reducing convective heat losses.

Figure 2 Parabolic trough concentrator (Carlos Antonio Pineda Arellano por, 2018)**.**

1.2.2 Fresnel reflectors

In contrast, Linear Fresnel Reflector systems (Figure 3) use an array of flat or slightly curved mirrors that reflect solar radiation toward a fixed linear receiver. A secondary optical concentrator near the receiver often intensifies the solar flux, achieving a high radiation density on the absorber surface (Carlos Antonio Pineda Arellano, 2018). While LFR technology offers distinct advantages, the variety of commercially available designs remains limited. Its presence in the Mexican market is particularly scarce, representing an unexplored opportunity for development and application.

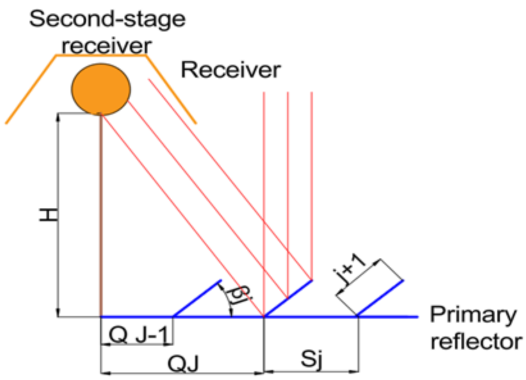

Figure 3 Schematic of a Linear Fresnel reflector system

1.3 Fresnel concentrators on the market

The variety of commercially available Fresnel concentrators remains limited, and their presence in Mexico is minimal due to a lack of local familiarity and development.

For instance, the Chromasun Micro Concentrator (MCT), marketed in the United States, achieves temperatures up to 200°C and measures 3390 mm × 1230 mm, as shown in Figure 4 (Chromasun Inc, 2011). This system serves applications such as air conditioning, hydronic heating, domestic hot water, process heating, and low-pressure steam generation.

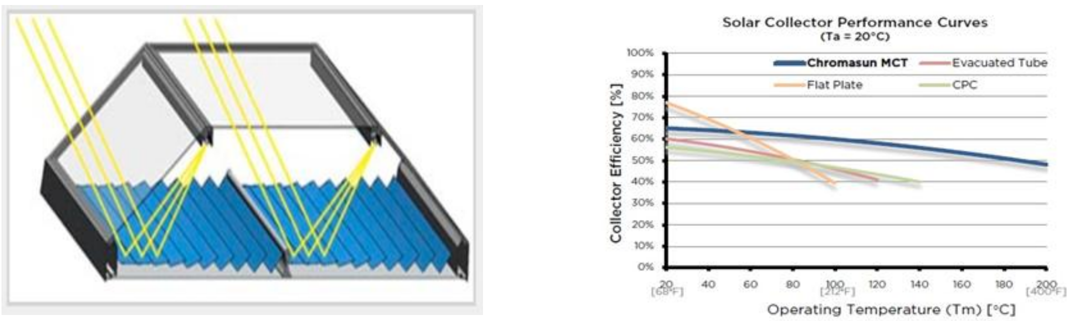

(A) MCT schematic view.

(b) MCT efficiency curve.

Figure 4 Chromasun Figures of Merit (Chromasun Inc, 2011)**.**

Similarly, the Solatom FLT20XL concentrator, marketed in Spain, operates at temperatures between 80°C and 300°C. It has dimensions of 6.8 m x 5.8 m x 3.5 m as seen in the Figure 5 and uses steam, water, or thermal fluid as a working medium.(Solatom CSP S.L, 2021).

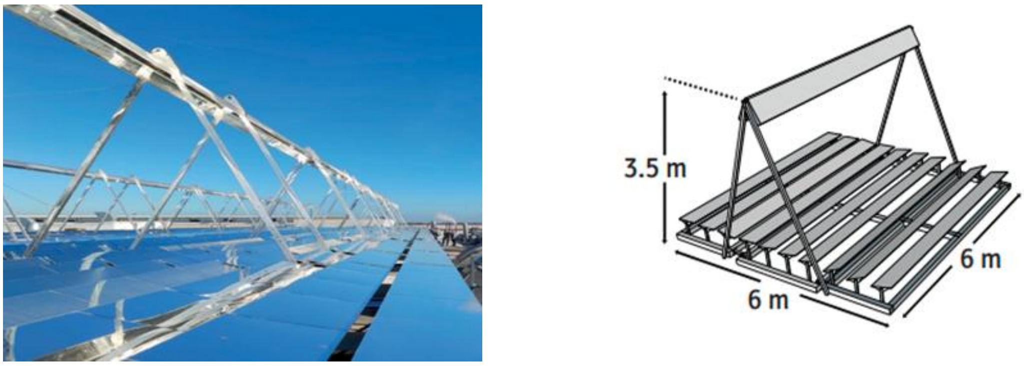

(a) Photograph of the Fresnel concentrator **(b) Schematic of the Fresnel**

Figure 5 Figuras de mérito del concentrador Solatom (Solatom CSP S.L, 2021)

Our literature review confirms that few Fresnel concentrator prototypes achieve temperatures of 300°C, and most target industrial process heat. The identified commercial devices are primarily located outside Mexico, which entails significant import costs. Table 2 summarizes key studies on Fresnel concentrators, providing a foundational basis for our research aimed at achieving the target temperature.

Table 2 Comparison between Fresnel concentrators and results with other authors

Autor	Receiver	Mirror area, (m2)	Temperature, (°C)	Thermal power, (W)
Ghod Bane et al. (Ghodbane et al., 2020)	Trapezoidal with parallel tubes	1.65	57-97	____
Abdelhamid Fadhel(Fadhel et al., 2023)	Galvanized pipe	0.89	50-97	____
Pablo Dellicompagni ulino(Dellicompagni et al., 2024)	Trapezoidal with parallel tubes	1.44	60-80	2000 ≥ 5000
Gutiérrez - Javier, P. (Gutiérrez Javier y Palacios Rolando, 2018)	Vacuum evacuated tubes	10.5 m2	80 - 120	890 W
SunDial de ASTEP (Rovira).	____	____	175-200	____
Project UAEMex	Copper tube	____	100-300	

2. Materials and methods

The methodology of the present paper is shown in Figure 6. In this work, We begin with an analysis of the energy consumption of Mexican industries, focusing on process-heat, compiled by INEGI (National Institute of Statistics and Geography)(INEGI, 2014). This analysis confirmed that over 50% of the thermal demand falls within the 100 °C to 300 °C range. We then performed a detailed geometric and optical characterization of a previous Fresnel reflector prototype, measuring key parameters including mirror spacing, mirror-receiver separation, receiver diameter, and intercept factor. Based on these measurements, we generated candidate receiver cavity geometries: trapezoidal and a faceted design based on compound parabolic concentrator (CPC) profiles.

We imported each design into SolTrace (Wendelin, 2003) to simulate ray trajectories, which enabled us to optimize mirror alignment, adjust receiver height, and evaluate critical performance metrics such as intercept factor, flux distribution uniformity, and overall optical efficiency. The CAD model was iteratively refined through simulation until the design achieved the targeted efficiency values. Some important parameters for optimizing a Fresnel solar concentrator are the separation, width of the mirrors, and the height of the receiver. Too small a separation can cause shading or blockage between the mirrors, which decreases the system efficiency. The width of the mirrors must be adequate to ensure that the reflected light is properly concentrated on the receiver. Meanwhile, the height of the receiver must be defined to capture the greatest possible amount of radiation; the inclination of each mirror improves the capture of solar rays. Furthermore, the use of a second cavity can significantly contribute to increasing system efficiency. Finally, the angles of incidence and reflection are essential to ensure that the solar rays interact correctly with the primary mirrors and are effectively directed toward the receiver.

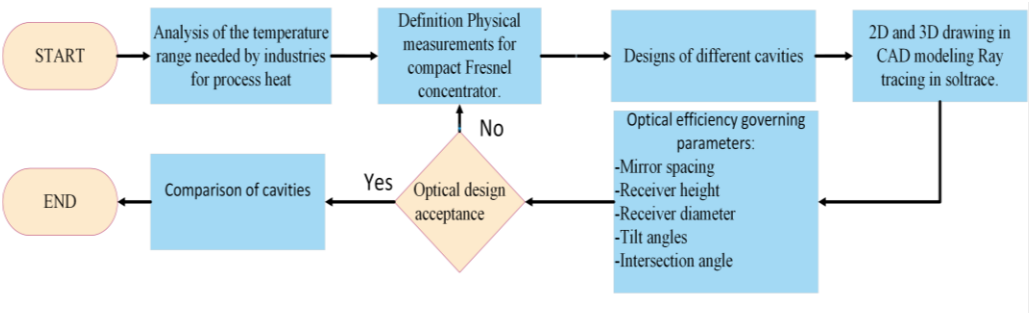

Figure 6 Proposed design methodology.

2.1 Preliminary design parameters

Figure 7 presents a simplified schematic of a generic linear Fresnel collector. The angle of incidence is the angle between the collector's reference direction—conventionally the zenith axis for normal incidence—and the nominal direction of the incoming solar rays. For linear Fresnel collectors, this angle resolves into two components in orthogonal planes: the transverse plane and the longitudinal plane, as illustrated in Figure 8. The transverse plane is perpendicular to the linear axis of the reflectors (y-axis), while the longitudinal plane is parallel to it. Consequently, the sun's position is uniquely defined by a combination of these transverse and longitudinal incidence angles. The geometric configuration of a linear Fresnel collector is characterized by several parameters, as detailed in Table 3.

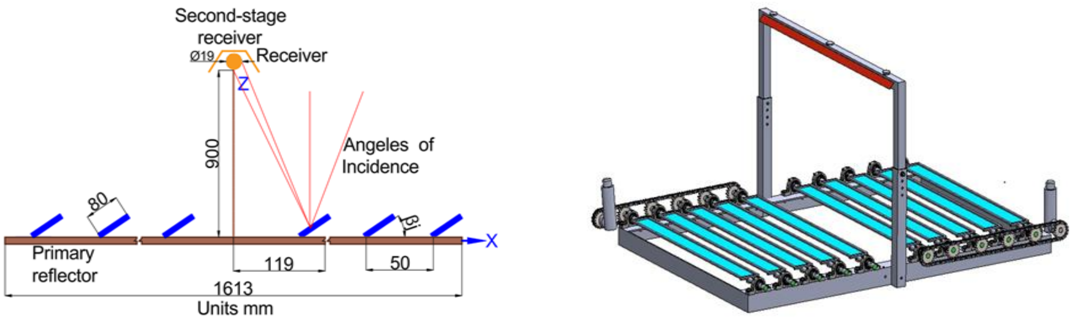

Figure 7 LFR schematic design, and 3D CAD view.

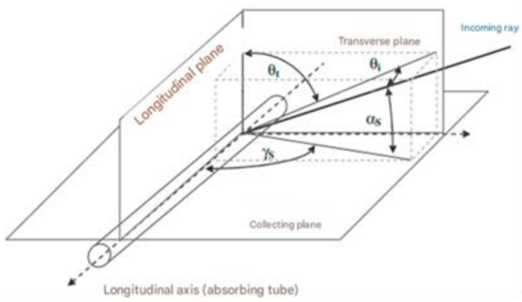

Figure 8 Definition of angles of incidence (Morin et al., 2012)

Table 3 Parameters for the LFR design

Parameter	Value
Number of mirrors	10 pieces
Spacing between mirrors, (mm).	50
Shape of the mirrors.	Plate
Mirror width, (mm).	80
Receiver assembly height, (mm).	900
Receiver size, (mm).	19
Receiver geometry	Circular
Cavity	Trapezoid, CCP, linearized non-imaging optics
Distance to the first mirror, (mm).	119
Length of each mirror, (mm).	1000

2.2 CPC Cavity Design

The unmodified Compound Parabolic Concentrator (CPC) design proposed by Winston adheres to the parametric equations provided in Eq. (1). In a modified CPC configuration, the rays no longer redirect tangentially to the absorber surface but instead intersect it secantly. This deviation necessitates a methodological adjustment to accommodate the absorber separation. As depicted in Figure 9, displacing the absorber requires a corresponding modification of the involute profile. Specifically, for a distance $g = r_2 - r_1$, the involute must undergo a rotation by an angle β_1, initiating the trace when $X_2 = 0$. The resulting rotated involute profile is defined by Eq. 3. Similarly, the macrofocal parabola of the CPC must be rotated as shown in Eq. 4.

$$\begin{cases} X_1 = \rho \cos t - r \sin t \\ X_2 = -(\rho \sin t + r \cos t) \end{cases} \qquad \text{(eq. 1)}$$

$$\beta 1 = \sqrt{\left(\frac{r_2}{r_1}\right)^2 - 1} - arccos\frac{r_1}{r_2} \qquad \text{(eq. 2)}$$

$$AB: \rho_0 = r(t + \beta 1), arcos\left(\frac{r_1}{r_2}\right) \leq t \leq \frac{\pi}{2} + \theta_0 \qquad \text{(eq. 3)}$$

$$BC: \rho_o = \frac{r_1\left[t + \theta_0 + \frac{\pi}{2} + 2\beta_i - cos(t - \theta_0)\right]}{1 + sin(t - \theta_0)} \quad , \quad \frac{\pi}{2} + \theta_0 \leq t \leq \frac{3\pi}{2} - 3\theta_0 \qquad \text{(eq. 4)}$$

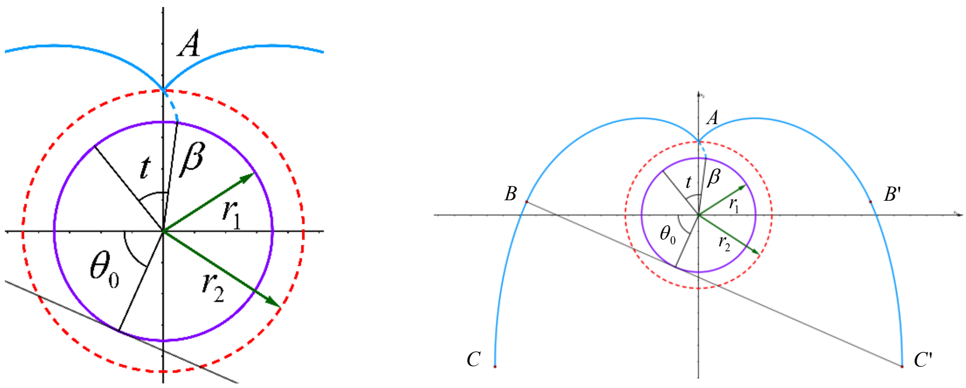

Figure 9 Displacement of the absorber from the involute (González-Mora and Dolores Durán García, 2020)

2.3. Cavities analysed.

Cavity design plays a critical role in optimizing the performance of LFR systems. The cavity, defined as a partial or complete enclosure surrounding the receiver tube, functions to minimize convective and radiative heat losses while maximizing solar radiation absorption. To develop effective cavity geometries, we utilize an involute-based design methodology, applying the parametric equations and rotated involute formulations detailed in the previous section. This approach enables the proposal of multiple cavity models. We have selected three specific designs for further evaluation, primarily due to their manufacturing simplicity and cost-effectiveness, while consistently adhering to the rotated involute profiles depicted in Figure 10.

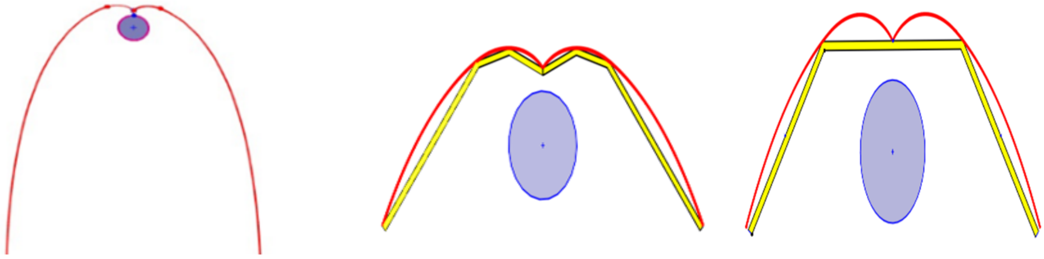

(A) CPC-Cavity **(B) M-Cavit (linearized non-imaging opticsa)** **(B) T-Cavity**

Figure 10. Cavities analyzed in the present study.

2.3 Ray tracing procedure

The ray-tracing procedure, illustrated in Figure 11, follows a systematic process. It begins by defining the solar position coordinates, which can be input as global coordinates or specific parameters such as latitude, date, and time. Then, the solar shape model is selected: Gaussian, pillbox, or a user-defined profile, to generate the angular distribution of incident rays.

The subsequent phase involves configuring the optical properties, where parameters such as reflectivity, transmissivity, and optical errors are specified for each component. The geometry is then defined; this study considers two distinct geometries: one for the primary mirror field and another for the receiver assembly, including the secondary cavity. At this stage, surface properties and apertures are set, and the optical behavior (refraction or reflection) is assigned. To ensure accurate solar alignment within the software, aim points for both axes must be defined for the primary mirrors and the secondary stage.

The core simulation phase, "TRACE," propagates a specified number of rays through the optical system. The chosen ray count, typically in the order of millions of rays for detailed flux mapping, directly influences the accuracy of the results and computational time. During this interaction stage, the software generates a 3D model from the predefined geometries, which can be visualized with or without ray paths.

Finally, the flux mapping stage presents the results. The interface displays a surface plot of flux intensity alongside a list of impacted elements. Key statistical outputs—including maximum, minimum, and average flux values—provide critical data for evaluating concentrator performance and guiding design optimization to enhance overall system efficiency.

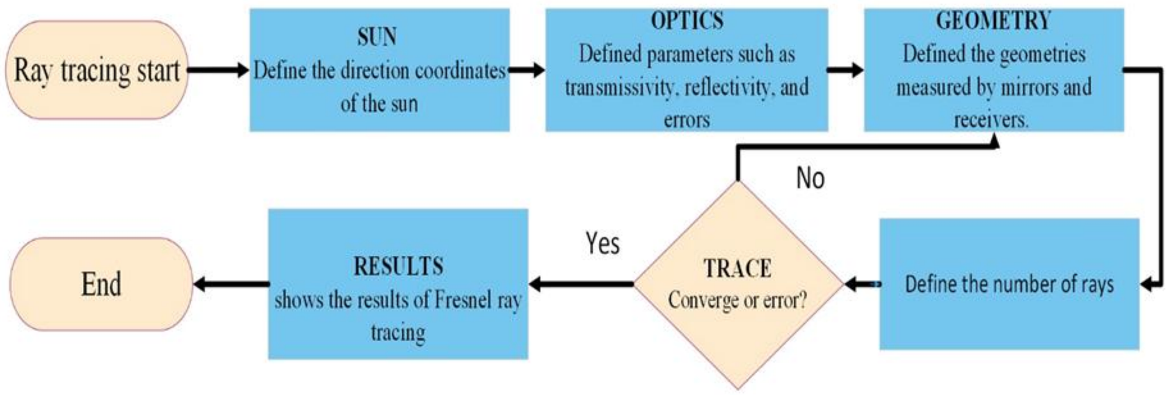

Figure 11 Ray tracing procedure.

Moreover, this analysis incorporates realistic conditions of sun shape and mirror optical errors (Santos et al., 2025). The ray-tracing simulation includes a slope error of 0.4 mrad, a specularity error of 0.1 mrad, and a pillbox sun shape of 4.65 mrad.

To compare LFR designs with different cavity configurations, we employ a metric termed the performance ratio (ξ_{pr}). This parameter quantifies the performance of each design relative to a UACM reference design, as defined by the following equation:

$$\xi_{pr} = \frac{\eta_{o,design}}{\eta_{o,UACM}} \quad \text{(eq. 5)}$$

This ratio facilitates a comparative analysis between design alternatives, enabling a systematic evaluation of optical efficiency improvements against the established benchmark. The calculation directly identifies which cavity design offers the highest efficiency, and which performs less effectively.

3. Results

In ray-tracing analysis, ensuring statistical convergence is critical for obtaining reliable results. We evaluated the convergence of five key parameters—peak flux, peak flux uncertainty, mean flux, mean flux uncertainty, and total receiver power—as functions of the number of rays traced (N). Figure 12 presents this statistical behavior, demonstrating that the values for all parameters stabilize beyond approximately 7×10^7 rays. This stabilization indicates that convergence has been achieved, thereby ensuring the consistency and validity of the simulation results for the evaluated design.

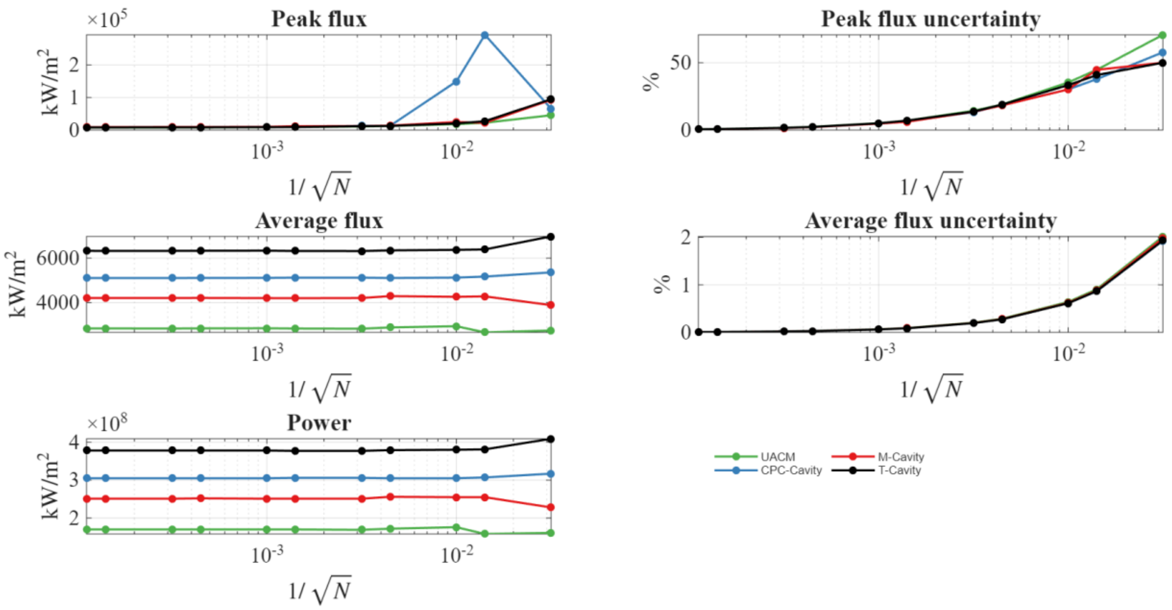

Figure 12 Ray-tracing convergence

Solar flux maps generated using SolTrace software visualize the spatial distribution of solar radiation on the receiver surface for the four cavity designs studied (Figure 13). Analysis of these maps reveals that the trapezoidal cavity achieves the highest optical efficiency. In these visualizations, the color scale ranges from yellow, indicating zones of peak flux intensity, to blue, representing areas of minimal energy concentration. This detailed flux distribution is critical for assessing optical performance, as it shows precisely where energy is concentrated on the receiver.

A key quantitative metric derived from this analysis is the average flux (kW/m^2), which is essential for calculating the system's overall optical efficiency and estimating the useful energy intercepted by the receiver. For clearer visualization of the flux pattern, the cylindrical receiver is presented as an unrolled, flat surface. This representation enables precise localization of the zones receiving the highest solar energy concentration. The corresponding optical efficiencies, calculated from the SolTrace output for a simulation using 5×10^6 rays, are compiled in Table 4. The data confirm that the trapezoidal cavity design is more efficient than the other cavity types evaluated.

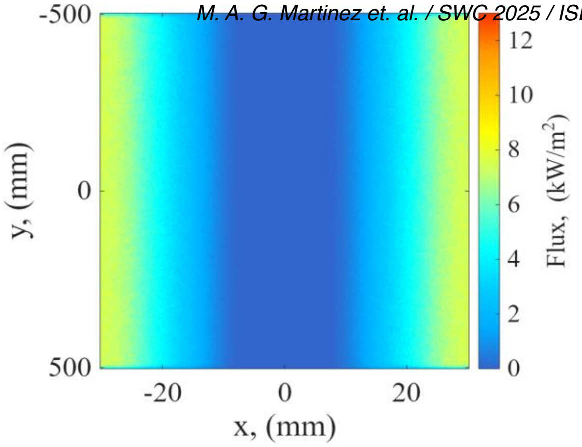

(a) UACM

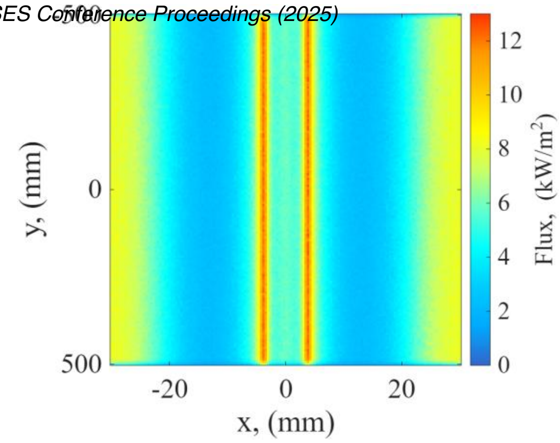

(b) CPC-cavity

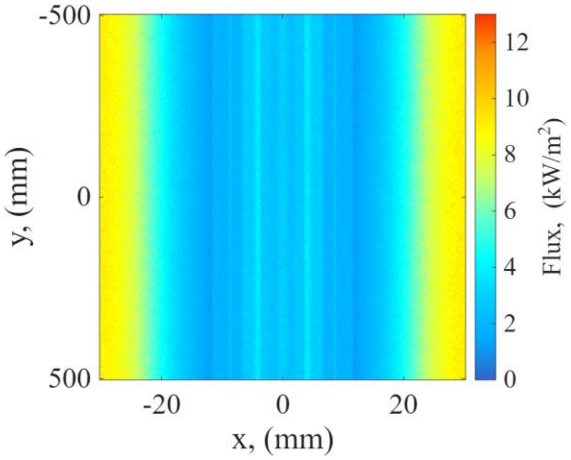

(c) M-cavity

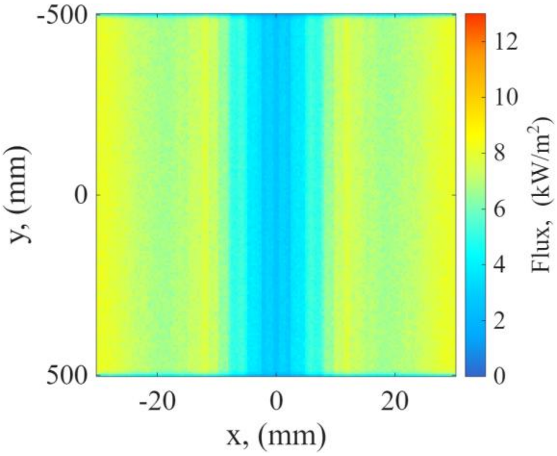

(d) T-cavity

Figure 13. Fresnel flux map for the 4 studies

Table 4 LFR designs performance comparison.

Parameter	UACM	CPC-Cavity	M-Cavity	T-Cavity
Peak flux, (kW/m^2)	7645.59	10723.2	9220.63	8354.79
Average flux, (kW/m^2)	2846.37	5109.49	4208.31	6327.79
Optical efficiency	0.11	0.20	0.17	0.25

The convergence analysis confirms the robustness of our simulation results, which reveal significant performance variations among the different secondary cavity designs. SolTrace simulations demonstrate that the trapezoidal cavity design outperforms both the Compound Parabolic Concentrator (CPC) and the non-imaging optics linearized (M-shaped) cavity configurations. We evaluated the optical performance by analyzing the transverse incidence angle modifier (IAM_t) for each cavity, which measures the fraction of radiation correctly concentrated on the receiver. An IAM_t value of 1 indicates no optical loss, values below 1 represent partial loss due to misdirection or reflection, and a value of 0 signifies no effective concentration.

The IAM_t behavior varies distinctly across cavities: the M-cavity achieves high efficiency at incidence angles of 20–30° but declines rapidly at higher angles, indicating acute sensitivity. The CPC cavity exhibits a smooth, stable decline in efficiency but maintains consistently lower performance. In contrast, the trapezoidal cavity effectively captures rays up to approximately 58°. The reference UACM design retains high IAM_t values up to 40° before dropping abruptly to zero, revealing non-uniform performance. Despite its initial high values, the UACM design's overall efficiency is inferior to the other cavities, as further detailed in.

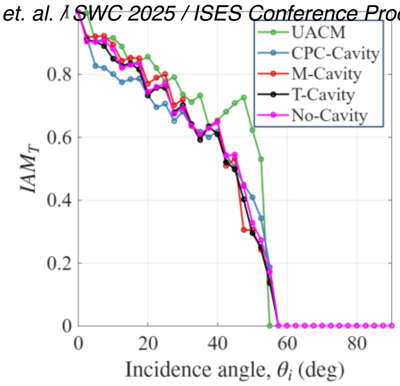

Figure 14 Incidence angle modifiers for transversal direction.

The longitudinal incidence angle modifier (IAM_l) curve for the non-imaging linearized (M) cavity and the trapezoidal cavity shows a gradual decline, maintaining an IAM_l value greater than 0.8 across a wide angular range due to their ideal cavity design. In contrast, the CPC cavity performance decreases more rapidly beyond 20–30°. The UACM design and a configuration with no cavity exhibit a useful operational range only up to approximately 25°, confirming that the newly proposed cavities deliver superior longitudinal performance.

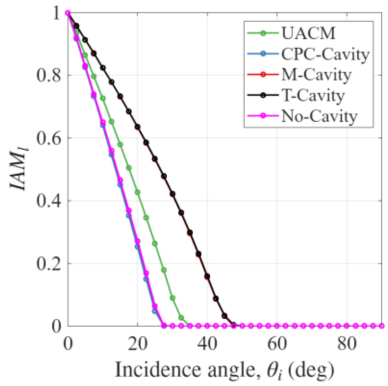

Figure 15 Incidence angle modifiers for longitudinal direction.

Analysis of the transverse incidence angle modifier (IAM_t) plots indicates that our cavity designs operate on a different principle than the UACM reference, which lacks a secondary cavity. However, evaluation of the performance ratio (ξ_{pr}) in Figure 16 demonstrates that the proposed cavities exceed the efficiency of the UACM design. This confirms that the cavities are functioning correctly, with the trapezoidal cavity exhibiting the highest efficiency. The trapezoidal design also offers advantages for manufacturing, as its geometry promises easier and more cost-effective fabrication compared to the more complex selective manufacturing and material requirements of other cavities, which would increase cost.

These findings underscore the critical importance of cavity geometry, mirror spacing, and receiver position. Optimizing these parameters creates an aperture that maximizes ray capture while uniform mirror spacing prevents shading and blocking. Collectively, these design optimizations enable a small-scale linear Fresnel concentrator to achieve optical efficiencies comparable to larger industrial systems, while maintaining low operating costs and a compact footprint.

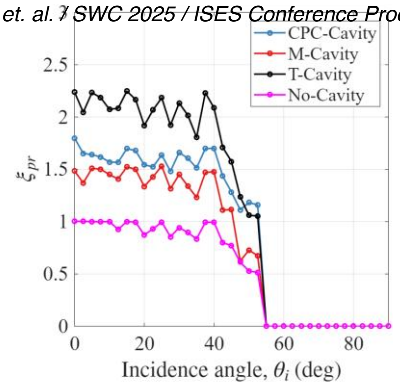

Figure 16 Performance ratio

4. Conclusion

This study aimed to develop and optically characterize a compact Linear Fresnel Reflector (LFR) optimized for industrial process heat. We pursued this goal by designing and evaluating several secondary receiver cavities, employing a robust methodology centered on Monte Carlo ray-tracing simulations in SolTrace. Our approach systematically compared different cavity geometries a trapezoidal design, a compound parabolic concentrator (CPC) based design, and a non-imaging linearized (M) cavity against a reference UACM design that lacked a secondary cavity.

We demonstrated that the trapezoidal cavity design delivers superior optical performance, exhibiting the highest optical efficiency and the most uniform flux distribution on the receiver surface. The performance ratio (ξ_{pr}) analysis and incidence angle modifier (IAM) curves confirm that this cavity maintains high optical efficiency across a wider range of incidence angles compared to all other configurations. A primary limitation of this study is its reliance on simulation data; while we ensured statistical convergence, experimental validation under real-world conditions is necessary to confirm these numerical findings.

Our findings significantly advance the design of small-scale LFR systems by quantitatively linking specific geometric parameters such as cavity shape, mirror spacing, and receiver height to overall optical performance. The trapezoidal cavity's superiority, coupled with its inherent manufacturability and cost-effectiveness, presents a practical solution that outperforms the more complex CPC-based designs often discussed in literature. For future work, we recommend constructing and testing a physical prototype to validate the simulated thermal performance and assess long-term operational reliability. Subsequent research should also investigate the system's economic viability and its integration with thermal storage to ensure continuous operation.

This framework, the context design was analyzed to show that the trapezoidal cavity presents a high performance that allows significant progress in the optimization of the compact linear Fresnel concentrator. The study provides a practical and efficient solution for generating medium-temperature process heat, directly addressing the challenge of industrial decarbonization. By demonstrating a path toward cost-effective and locally manufacturable solar concentrators, this work contributes to making renewable thermal energy a more accessible and viable alternative for a significant portion of global energy demand.

5. Acknowledgments

Marco Antonio González Martínez gratefully acknowledges the financial support provided by SECIHTI (Master's grant CVU: 2056021) and COMECyT (Grant: 2025-2EA3209).

6. References

Carlos Antonio Pineda Arellano por, A., 2018. Diseño de un concentrador Fresnel de foco lineal para aplicaciones de calor de proceso. Centro de investigaciones en óptica, A.C.

Chromasun Inc, 2011. chromasun. [WWW Document]. URL http://chromasun.com/ (accessed 9.26.24).

Dellicompagni, P., Gulino, S., Perello, D., Trigo, M., 2024. Caracterización experimental de un concentrador solar Fresnel lineal. Revista Científica de la UCSA 11, 3–18. https://doi.org/10.18004/ucsa/2409-8752/2024.011.01.003

Fadhel, A., Eddhibi, F., Charfi, K., Balghouthi, M., 2023. Investigation of a Linear Fresnel solar collector (LFSC) prototype for phosphate drying. Energy Nexus 10. https://doi.org/10.1016/j.nexus.2023.100188

Fred A. Curtis, 1984. Energy Developments: New Forms, Renewables, Conservation. Elsevier. https://doi.org/10.1016/C2013-0-05945-2

Ghodbane, M., Benmenine, D., Khechekhouche, A., Boumeddane, B., 2020. Brief on solar concentrators: Differences and applications. Instrumentation Mesure Metrologie 19, 371–378. https://doi.org/10.18280/i2m.190507

González-Mora, E., Dolores Durán García, M., 2020. Methodology for an opto-geometric optimization of a linear Fresnel reflector for direct steam generation. Energies (Basel) 13. https://doi.org/10.3390/en13020355

Gutiérrez Javier y Palacios Rolando, 2018. Desarrollo tecnológico de un concentrador solar lineal tipo Fresnel.

INEGI, 2014. INEGI, Censos económicos 2014, [WWW Document]. http://www.inegi.org.mx/est/contenidos/proyectos/ce/ce2014/default.aspx.

Morin, G., Dersch, J., Platzer, W., Eck, M., Häberle, A., 2012. Comparison of Linear Fresnel and Parabolic Trough Collector power plants. Solar Energy.

Payback MÉXICO, S., 2018. CALOR SOLAR PARA LA INDUSTRIA.

Rovira A, Abbas R, Jp, S., Barnetche M, Ibarra M, Barbero R, n.d. PROYECTO ASTEP: ESTADO Y PROGRESO HASTA 2024.

Santos, A.V., Canavarro, D., Horta, P., Collares-Pereira, M., 2025. On optimum designs of linear Fresnel solar collectors. Solar Energy 300. https://doi.org/10.1016/j.solener.2025.113852

Solar Payback, 2017. EL CALOR SOLAR INDUSTRIAL COMPENSA.

Solatom CSP S.L, 2021. solatom.com [WWW Document]. https://solatom.com/.

Tasmin, N., Farjana, S.H., Hossain, M.R., Golder, S., Mahmud, M.A.P., 2022. Integration of Solar Process Heat in Industries: A Review. Clean Technologies. https://doi.org/10.3390/cleantechnol4010008